Self-assembly in binary phospholipids mixtures

Summer School on Neutron Small Angle Scattering and Reflectometry
NIST Center for Neutron Research
June 26-30, 2006

Abstract

Mixtures of long and short tail lipids dissolved in solution have been purported to be useful for aligning proteins in solution to aid in structural NMR characterization as well as being potential media for membrane protein crystallization. Small-angle neutron scattering (SANS) will be used to characterize the structures formed by such mixtures at low temperature. Selective deuteration will then be used to elucidate the details of the internal structure of the objects formed. All aspects of the experiment, from the sample preparation and instrument setup through to the data treatment and interpretation will be briefly described and references given for more in-depth study.

I. INTRODUCTION

Phospholipid systems comprising mixtures of long and short chain lipids have received considerable attention in the last few years due to their unique combination of biocompatibility and of strong orientational properties in magnetic fields. This has lead to their importance as alignable liquid crystalline media for nuclear magnetic resonance (NMR) based protein structure determination and studies of membrane associated peptides and proteins [1,2], in which applications they have largely replaced lipid based vesicles and detergent based micellar systems. These useful properties have been attributed to the formation of self-assembled structures of "bicelles" in these mixtures of a bilayer forming long tail lipid and a micelle forming short tail lipid. More recently it was also demonstrated that the proton pump trans-membrane protein bacteriorhodopsin[3] could be crystallized from suspension in these lipid mixtures. These systems could therefore also play an important role in the production of the crystals needed for high resolution scattering determination of transmembrane protein structures, which to date despite their biological importance constitute only a tiny fraction of those reported in the Protein Data Base[4]. Understanding of the phase diagram of these lipid mixtures should therefore initially furnish a better background for interpretation of NMR results, but could in the future be crucial for systematically tailoring their properties to the goal of crystallizing specific membrane proteins.

Self-assembled structures have actually been postulated in a variety of lipid mixtures, both charged and neutral over wide ranges of temperatures. The most widely studied of these systems is the mixture of the 14-C chain phospholipid Dimyristoyl-phosphatidylcholine (DMPC) and the shorter 6-C chain Dihexanolyl-phosphatidylcholine (Figure 1). Several studies using spectroscopic techniques like nuclear magnetic resonance (NMR) and light and neutron scattering techniques have been published on these mixtures, yet they continue to be the subject of considerable scientific debate [Katsaras, Marcotte]. Dilute solutions of pure DMCP are well known to form vesicle while pure solutions of DHPC form micelles (Figure 2).

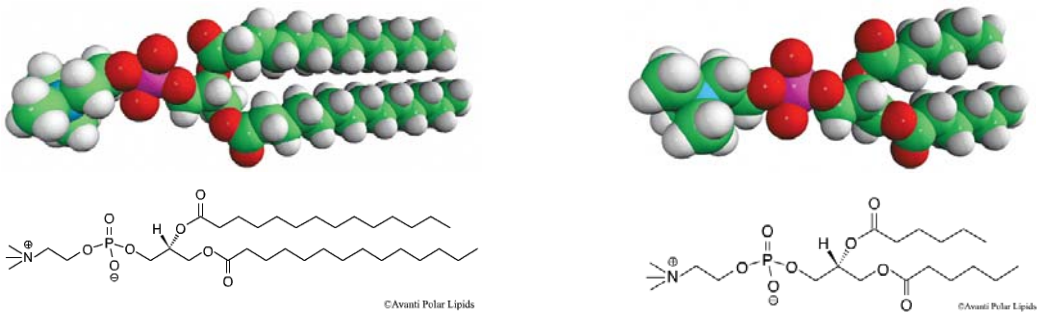

Figure 1: DMPC and DHPC structure

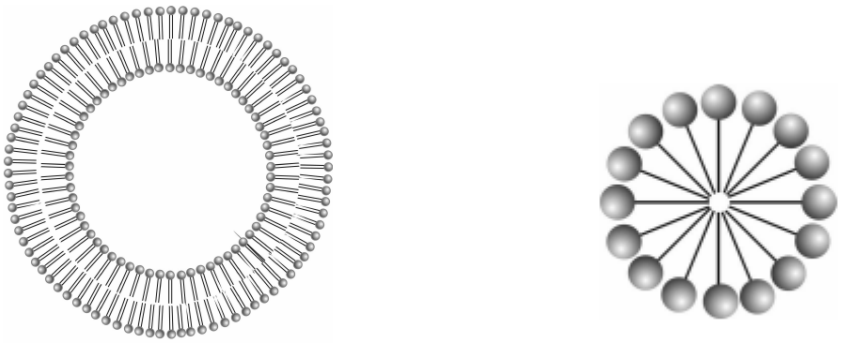

Figure 2: Schematic of DMPC vesicle and DHPC micelle structure

We propose in this experiment to characterize and determine the structure of the a zwitterionic lipid mixture with a long to short chain lipid molar ratio of q = [DMPC]/[DHPC] = 3 and a total lipid concentration of 50 mg/ml. Using selective deuteration of one of the lipids, we will then elucidate the details of the internal structure of the self-assembled aggregate.

The Objectives of the Experiment are:

- **To determine the average dimensions of the self-assembled aggregate**. This information will be derived from a Guinier analysis of the scattering at low Q.

- **Determine the volume fraction of the dispersed aggregate**. This information may be derived from the Q→ 0 limit of the scattering curve having scaled the data to absolute units of cross section per unit volume and from Porod's Invariant.

- **Determine, possibly, the presence or absence of inter-particle self-organization effects.** This will be done by identifying and analyzing deviations in the Q-dependence of the scattering from that expected for a non-interacting, dilute suspension of particles.

- **Determine the surface area from the Porod regime.** This will be done by analyzing the high Q regime.

- **Determine the shape of the self-assembled aggregate.** This will be done by analyzing the scattering curves with different models.

- **Determine the internal structure of the self-assembled aggregate.** This will be done by using selective deuteration in order to highlight only one lipid in the lipids mixture.

- **Characterize the morphology of the lipid mixture.** This will be performed by fitting simultaneously scattering curves from mixtures of hydrogenated and deuterated lipids.

II. PLANNING THE EXPERIMENT

Why use SANS?

Generally, static light scattering and small angle X-ray scattering (SAXS) provide the same information about the sample: measurement of the macroscopic scattering cross-section $d\Sigma/d\Omega(Q)$. The contrast in light scattering arises from the difference in the light's refractive index for each phase in the sample. The contrast in light scattering is typically much stronger than in SANS, requiring very dilute concentration of particles to avoid multiple light scattering. In addition, the wavelength of light limits $q < 0.002$ Å^{-1}. Thus light scattering can be used to estimate the diameter of large vesicle in dilute solution, but can not resolve the thickness of the lipid bilayer nor the size of the micelle (radius~2-5 nm). The contrast in X-ray scattering arises from the variation in electron density between the phases. The contrast is again stronger for X-rays than neutrons, but thinner samples often mitigate any multiple scattering. X-rays are strongly absorbed by most samples, requiring thin walled glass capillaries to contain the sample. Also, intense X-rays beams can cause irreversible sample damage altering the structure and chemistry of the studied solution. This is especially the case for organic compounds such as polymers, lipids and surfactants. In the present case, SAXS can be used to measure the data over the entire Q-range needed for this experiment and determine the size and shape of the self-assembled lipids mixture. However, characterization of the internal structure would be extremely difficult (or simply impossible) and would require much more complexity in modeling data.

Given the stated objectives of the experiment and the decision to use neutrons, how do we go about preparing for the experiment to maximize our chances of success? Here we discuss some of the issues that bear on this question.

II.1 Scattering Contrast

In order for there to be small-angle scattering, there must be scattering contrast between, in this case, the lipid mixture and the surrounding solvent (water). The scattering is proportional to the scattering contrast, $\Delta\rho$, *squared* where

$\Delta\rho = \rho_p - \rho_w$ ← Scattering Contrast

and ρ_p and ρ_w are the **scattering length densities** (**SLD**) of the "particles" and the water, respectively. Recall that **SLD** is defined as

$$\rho = \frac{\sum_{i=1}^{n} b_i}{V}$$ ← Scattering Length Density

where V is the volume containing *n* atoms, and b_i is the (bound coherent) **scattering length** of the i^{th} atom in the volume V. V is usually the molecular or molar volume for a homogenous phase in the system of interest.

The **SLDs** for the two phases studied here, lipids and water, can be calculated from the above formula, using a table of the scattering lengths (such as Ref. 5) for the elements, or can be calculated using the interactive *SLD Calculator* available at the NCNR's Web pages (http://www.ncnr.nist.gov/resources/index.html). The **SLDs** for DHPC, DMPC, d_DMPC, d_DHPC and water (both H_2O and D_2O) are given below in Table 1.

Table 1. The scattering length densities (SLDs) for DMPC, DHPC, d_DMPC, d_DHPC light water and heavy water.

Material	Chemical Formula	Mass Density (g/cc)	SLD (cm^{-2})
DMPC	$C_{36}H_{72}NO_8P$	1.074	0.29×10^{10}
DHPC	$C_{20}H_{40}NO_8P$	1.14	0.67×10^{10}
d_DMPC	$C_{36}H_5D_{67}NO_8P$	1.378	8.11×10^{10}
d_DHPC	$C_{20}H_5D_{35}NO_8P$	1.3	6.55×10^{10}
Light water	H_2O	1.0	$-.56 \times 10^{10}$
Heavy water	D_2O	1.1	6.38×10^{10}

We see from Table 1 that the scattering contrast for an hydrogenated lipid mixture in D_2O [proportional to $(0.5 - (6.38))^2 \sim 34$] is ~ 34 times greater than in H_2O [$(0.5 - (-0.56))^2 \sim 1$]. Contrast between a deuterated lipid mixture in H2O is [proportional to $(7.33 - (-0.56))^2 \sim 62$] is ~ 62 times greater than in D2O [proportional to $(7.33 - 6.38)^2 \sim 1$]. However, this is not the only factor to consider. One should take into account the price of the deuterated lipids which is ~1000 more expensive than the hydrogenated counterpart. Even if one does not have any budget restriction, one should also consider the incoherent scattering from each phase[a]. The incoherent scattering contributes to an isotropic background that can obscure weak coherent scattering from the smaller structural features in a material. Here we are interested in both small-scale structure and much larger scale structure. Since the incoherent scattering from H_2O is about 30 times greater than that from D_2O, we elect to do the experiment using D_2O as the solvent. The contrast in D_2O is quite adequate and the lower incoherent scattering background will make it easier to distinguish the Q-dependent coherent signal from the Q-independent

[a] Incoherent neutron scattering has no counterpart in x ray or light scattering. It arises from the interaction of the neutron with the nucleus, which is described by a scattering length that depends on the particular nuclear isotope and its nuclear spin state. For more information, see, for example, Ref. 5

incoherent background. In addition, the lower incoherent scattering from D_2O allows us to use a thicker sample, as we shall see next.

II.2 Sample Thickness

The next decision we face is how thick should the sample be? Recall that the scattered intensity, $I_s(Q)$, is proportional to the product of the sample thickness, d, and the sample transmission, T_s, where T_s, the ratio of the transmitted beam intensity to the incident beam intensity, is given by

$$T_s = e^{-\Sigma_t d}, \quad \Sigma_t = \Sigma_c + \Sigma_i + \Sigma_a$$

where the total cross section per unit sample volume, Σ_t, is the sum of the coherent, incoherent and absorption cross sections per unit volume. The absorption, or neutron capture, cross section, Σ_a, can be computed accurately from the tabulated absorption cross sections of the elements (and isotopes) if the mass density and stochiometry of the phase is known. Σ_a is wavelength dependent, being linearly proportional to λ for nearly all elements. The incoherent cross section, Σ_i, can be *estimated* from the cross section tables for the elements as well, but not as accurately because it depends somewhat on the atomic motions and is, therefore, temperature dependent. The coherent cross section, Σ_c, can also only be estimated since it depends on the details of both the structure and correlated motion of the atoms in the material.

The computations involved in estimated sample transmission are straightforward but tedious. The task is made easier using the NCNR's Web-based *SLD calculator* which computes not only scattering length density, but also estimates the incoherent and absorption cross sections per unit volume. Table 2 gives some of these results for the different lipids, H_2O and D_2O.

Table 2. Macroscopic cross sections (i.e. cross sections per unit volume) computed with the ***SLD calculator*** on the NCNR's Web site for the solute and solvents in the experiment. The values for the absorption cross sections are for a wavelength of 6 Å.

	Σ_c (cm^{-1})	Σ_i (cm^{-1})	Σ_a (6 Å) (cm^{-1})	Σ_t (cm^{-1})	$1/\Sigma_t$ (cm)
DMPC	~0	5.87	0.0831	5.9524	0.168
DHPC	0.0131	5.2	0.0779	5.291	0.189
d_DMPC	0.0011	0.674	0.0145	0.6896	1.45
d_DHPC	0.0035	0.861	0.0204	0.8849	1.13
H_2O	0.260	5.37	0.0741	5.70	0.175
D_2O	0.518	0.136	0.000135	0.654	1.53

The sample to be measured consists of approximately 5 % hydrogenated lipid (by weight) in D_2O, or ~0.05 % lipid by volume. Hence the total cross section per unit volume for the suspension is 0.95 (0.654 cm^{-1}) + 0.05 (5.5 cm^{-1}) = 0.896 cm^{-1}, and $1/\Sigma_t$ = 1.11 cm.

Hence the optimal sample thickness[b], the 1/e thickness, is 1.11 cm. The corresponding thickness for the same volume fraction of either hydrogenated or deuterated lipid in H_2O is ~0.175 cm. Hence the large incoherent cross section of hydrogen not only contributes a significant Q-independent background, it also limits the optimal sample thickness.

II.3 Required Q-Range

For this experiment we know we will need to measure the intensity over a wide Q-range since the information we are looking for is distributed in the low and high Q regime. To get a better idea of the required Q-range, we can use the *SANS Data Simulator* (http://www.ncnr.nist.gov/resources/simulator.html) to calculate the Q-dependence of the scattering for the case of non-interacting and randomly oriented monodisperse spherical particle. From among the 20 different particle models currently included in the *SANS Data Simulator*, we choose the *Sphere* model (the simplest model we have). The documentation for this model can be found on the Web site at http://www.ncnr.nist.gov/resources/sansmodels/sphere.html. A plot from the *SANS Data Simulator* for monodisperse, randomly oriented sphere is shown in Fig. 3.

Notice in Fig. 3 that the scattering at larger Q is dominated by the solvent scattering from the solution. It will be necessary to correctly subtract this scattering curve in order to reveal the Q^{-4} power law characteristic of sharp interfaces.

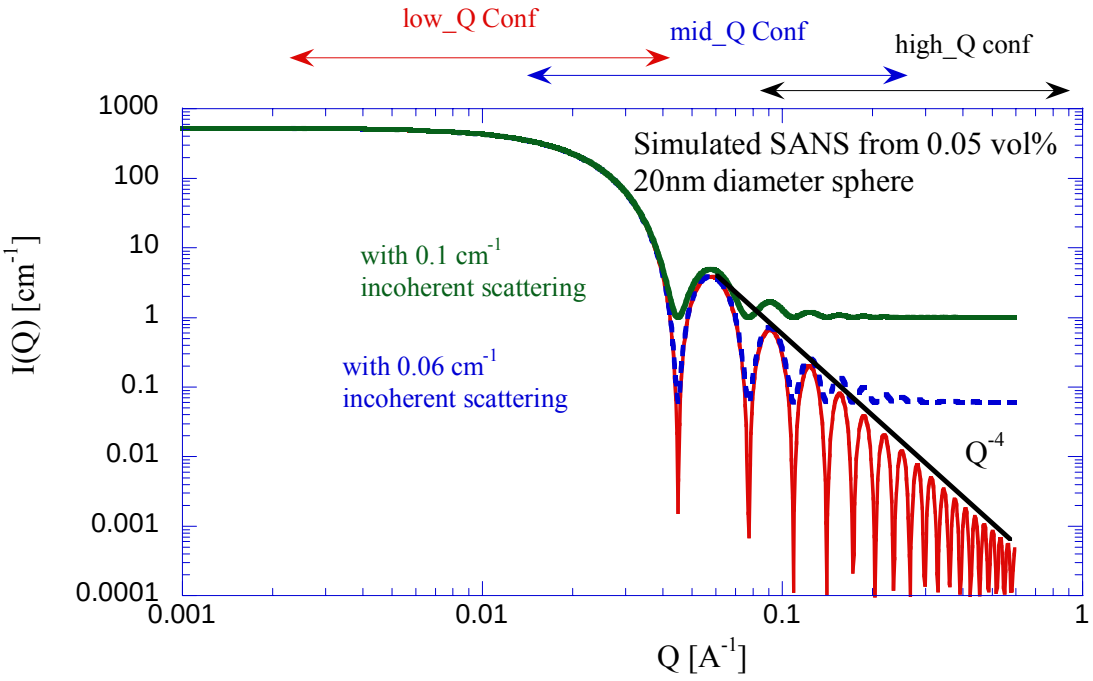

[b] The scattered intensity is proportional to $d \exp(-\Sigma_t d)$ which has a maximum at $d = 1/\Sigma_t$. However, if Σ_i and Σ_a are small compared with Σ_c, d should be chosen to make T ~ 0.9 rather than 1/e = .37 to avoid multiple scattering.

Figure 3. The simulated SANS from monodisperse, randomly oriented sphere with diameter D = 20 nm. The dash curves include the incoherent scattering from the different solvent (D_2O and H2O solvent).

III. COLLECTING THE DATA

III.1 How to Configure the SANS Instrument

Now that we know we want to cover as wide a Q-range as possible, we must decide how to configure the SANS instrument to do so efficiently. Here again we can use a computational tool, called SASCALC, as a guide. A schematic of the NCNR's 30-m SANS instruments is shown in Fig. 4, and the instrument configuration parameters, and their allowed range for the NG-7 30-m SANS instrument, are listed in Table 3.

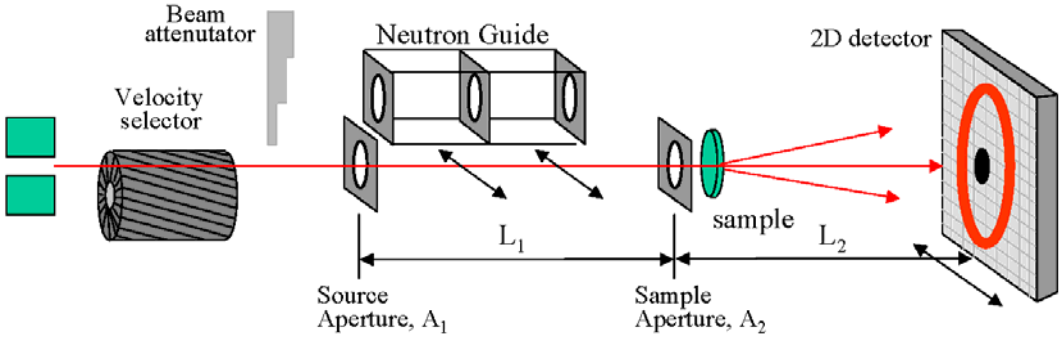

Figure 4. Schematic diagram of the components of the NCNR's 30-m SANS instruments.

Table 3. The instrument configuration parameters, and their range of allowed values, for the NG-7 30-m SANS instrument.

Variable	Allowed Values
Neutron wavelength	5 – 20 Å (determined by the rotational speed of the velocity selector)
Wavelength spread (FWHM)	0.09, 0.11 or 0.22 (determined by the inclination of the velocity selector axis with respect to the beam direction)
Number of neutron guides, Ng	0 – 8 (determines the beam collimation by changing the distance of the source aperture from the sample)
Source aperture diameter	1.43, 2.20 or 3.81 cm for Ng=0; 5.08 cm for Ng=1-8
Sample-to-detector distance (SDD)	100 – 1530 cm
Detector offset	0 – 25 cm (detector translation perpendicular to beam to extend the Q-range covered at a given SDD)
Sample aperture diameter	0 – 2.5 cm
Beamstop diameter	2.54, 5.08, 7.62 or 10.16 cm
Beam Attenuator	10 choices of beam attenuator thickness to reduce beam intensity for sample transmission measurements

For a given set of allowed parameters, SASCALC computes the corresponding Q-range and the beam intensity (n/sec) on the sample. The Q-range for a particular configuration is determined by the choice of wavelength, detector distance and detector offset. To reach the largest-Q limit of the instrument, the shortest available wavelength, 5 Å, the shortest sample-to-detector distance, 100 cm, and the maximum detector offset, 25 cm have to be used. The number of neutrons guides affects primarily the beam intensity on the sample. In general, we choose the largest number of guides, to maximize the beam intensity on the sample, consistent with the desired Q-range. In the present case, because of sample polydispersity and instrument resolution, the high Q regime is not very important and we will use the following SASCALC choice:

Instrument Configuration for large-Q portion of measurement range

Wavelength:	6.0 Å $\Delta\lambda/\lambda$: 0.11 (FWHM)
Number of guides:	8
Sample-to-Detector distance:	100 cm
Detector Offset:	20.00 cm
Intensity at sample:	2.987E+006 Counts/sec
Qmin:	**0.0318 Å^{-1}** Resolution: 23.4%
Qmax:	**0.5669 Å^{-1}** Resolution: 4.7%
Horizontal Qmax:	0.4974 Å^{-1}
Vertical Qmax:	0.323 Å^{-1}
Source aperture diameter:	5.08 cm
Sample Aperture diameter:	1.2 cm
Beam diameter at detector:	3.14 cm
Beamstop diameter required:	5.08 cm, (2.0 in)
Attenuator for transmission measurements:	No. 8
Source aperture to sample aperture distance:	387.0 cm

Next we consider how to configure the instrument to reach the low-Q end of the desired measurement range. In this experiment we want to reach low Q-values to observe the plateau the form factor. The Q-range and other parameters for this configuration are as follow:

Instrument Configuration for low-Q portion of measurement range

Wavelength:	6.0 Å $\Delta\lambda/\lambda$: 0.11 (FWHM)
Number of guides:	0
Sample-to-Detector distance:	1530 cm
Detector Offset:	0 cm
Intensity at sample:	1.7 E+5 Counts/sec
Qmin:	**0.0029 Å^{-1}** Resolution: 26.3%
Qmax:	**0.031 Å^{-1}** Resolution: 5.1%
Horizontal Qmax:	0.0219 Å^{-1}
Vertical Qmax:	0.0219 Å^{-1}
Source aperture diameter:	3.81 cm

Sample Aperture diameter:	1.2 cm
Beam diameter at detector:	6.37 cm
Beamstop diameter required:	7.62 cm, (3.0 in)
Attenuator to use for transmission measurements:	No. 5
Source aperture to sample aperture distance:	1627.0 cm

For this experiment we will need a third configuration to cover the gap between the low-Q and high-Q configurations (between Q ~ 0.016 $Å^{-1}$ and ~0.04 $Å^{-1}$). Here there are many combinations of wavelength and detector distance that will work. We now simply choose a detector distance that gives good overlap with the Q-ranges for the other two configurations. A detector distance of 400 cm will do this nicely. The output from *SASCALC* for this mid-Q configuration is:

Instrument Configuration for mid-Q portion of measurement range

Wavelength:	6.0 A $\Delta\lambda/\lambda$: 0.11 (FWHM)
Number of guides:	5
Sample-to-Detector distance:	400 cm
Detector Offset:	0 cm
Intensity at sample:	8.4 E+5 Counts/sec
Qmin:	**0.008 $Å^{-1}$** Resolution: 26.4%
Qmax:	**0.118 $Å^{-1}$** Resolution: 4.8%
Horizontal Qmax:	**0.0836 $Å^{-1}$**
Vertical Qmax:	**0.0836 $Å^{-1}$**
Source aperture diameter:	5.0 cm
Sample aperture diameter:	1.20 cm
Beam diameter at detector:	4.50 cm
Beamstop diameter required:	5.08 cm, (2.0 in)
Attenuator to use for transmission measurements:	No. 7
Source aperture to sample aperture distance:	852 cm

III.2 What Measurements to Make

In addition to measuring the scattering from the sample for the three instrument configurations described in the previous section, additional measurements are needed to correct for "background." Counts recorded by the detector with the sample in place can come from 3 sources: 1) neutrons scattered by the sample itself (the scattering we are interested in); 2) neutrons scattering from something other than the sample, *but which pass through the sample*; and, 3) everything else, including neutrons that reach the detector *without passing through the sample* (stray neutrons or so-called room background) and electronic noise in the detector itself. To separate these three contributions, we need three measurements:

i) Scattering measured with the sample in place (which contains contribution from all 3 sources listed above), denoted $\mathbf{I_{sam}}$;

ii) Scattering measured with the empty sample holder in place (which contains contributions from the 2nd and 3rd sources listed above), denoted $\mathbf{I_{emp}}$; and,

iii) Counts measured with a complete absorber at the sample position (which contains only the contribution from the 3rd source listed above), denoted $\mathbf{I_{bdg}}$.

In addition to these three 'scattering' measurements, the transmission (the fraction of the incident beam intensity that passes through the sample without being scattered or absorbed) of the sample and the sample cell must also be measured in order to correctly subtract the contributions to the background and to calibrate the scattering on an absolute cross section scale (the procedure is discussed in Section IV. Data Reduction). The transmission is measured by inserting a calibrated attenuator in the incident beam (to reduce the direct beam intensity to an accurately measurable level) and measuring the direct beam intensity with and without the sample (or the sample cell) in position. The ratio of these two short measurements (typically 1-2 minutes each) is the sample (or sample cell) transmission.

How the scattering and transmission measurements are used to reduce the data to a quantity, called the differential scattering cross section, that is intrinsic to the sample is described in Section IV. Data Reduction.

III.3 How Long to Count

A SANS experiment is an example of the type of counting experiment where the uncertainty, or more precisely the standard deviation, σ, in the number of counts recorded in time, *I(t)*, is $\sigma = \sqrt{I(t)}$. If the scattering is roughly evenly distributed over the SANS detector, then a good rule of thumb is that one should accumulate about 500,000 total detector counts per sample measurement. If the accumulated counts are circularly averaged, one obtains about 50 data points when plotting I(Q) versus Q. This amounts to about 1000 counts per data point with a standard deviation of $\sqrt{1000} \sim 30$ or an uncertainty of about 3 %, which is good enough for most purposes.

A related question, is how long should the background and empty cell measurements be counted relative to the sample measurement. The same $\sigma = \sqrt{I(t)}$ relationship leads to the following approximate result for the optimal relative counting times

$$\frac{t_{background}}{t_{sample}} = \sqrt{\frac{Count\ Rate_{background}}{Count\ Rate_{sample}}}\ .$$

Hence if the scattering from the sample is weak, the background should be counted for as long (but no longer!) as the sample scattering. However, if the sample scattering count rate is, say, 4 times greater than the background rate, the background should be counting only half as long as the sample scattering.

IV. DATA REDUCTION

Data reduction consists of correcting the measured scattering from the sample for the sources of background discussed in Section III.2, and multiplying the corrected counts by a scaling factor (to remove incidental differences between measurements such as the counting time and sample thickness) that puts the data on an absolute scale of scattering cross section per unit volume. The background-corrected neutron counts, $I_{cor}(Q)$, recorded in a detector pixel in a time interval t are related to absolute cross section, $d\Sigma(Q)/d\Omega$, through the expression

$$I_{cor}(Q) = \phi\ A\ \Delta\Omega\ \varepsilon\ t\ d\ T\ (d\Sigma(Q)/d\Omega), \qquad (1)$$

Where:

ϕ = the neutron flux (neutrons/cm^2-sec) at the sample
A = the area of the beam incident on the sample
d = the sample thickness
T = the transmission of the sample (and its container, if there is one)
$\Delta\Omega$ = the solid angle subtended by one pixel of the detector
ε = the detector efficiency, and
t = the counting time.

The incidental instrumental factors can be lumped together into one constant

$$K = \phi\ A\ \Delta\Omega\ \varepsilon\ t \qquad (2)$$

and the intrinsic quantity, $d\Sigma(Q)/d\Omega$, the differential scattering cross section per unit volume, is obtained by scaling the recorded counts

$$d\Sigma(Q)/d\Omega = I_{cor}(Q)/(\ K\ d\ T\ ) \qquad (3)$$

We now go over the specific steps involved in extracting $d\Sigma(Q)/d\Omega$ from the raw data. Following equation (1), the raw scattered intensity measured from the sample, I_{sam}, and the empty cell, I_{emp}, can be written as

$$\begin{aligned} I_{sam} &= K\ d\ T_{sample+cell}\left(\left(\frac{d\Sigma(Q)}{d\Omega}\right)_{sample} + \left(\frac{d\Sigma(Q)}{d\Omega}\right)_{emp}\right) + I_{bgd} \\ I_{emp} &= K\ d\ T_{cell}\left(\left(\frac{d\Sigma(Q)}{d\Omega}\right)_{emp}\right) + I_{bgd} \end{aligned} \qquad (4)$$

where $T_{sample+cell}$ and T_{cell} are the measured transmission of the sample (in its container) and the empty container, respectively. From the above, the background corrected scattering, denoted $\mathbf{I_{cor}}$, is given by

$$I_{cor} = (I_{sam} - I_{bgd}) - \left(\frac{T_{sample+cell}}{T_{cell}}\right)(I_{emp} - I_{bgd}) \qquad (5)$$

The corrected counts, I_{cor}, are proportional to the quantity of interest, namely the differential scattering cross section. From the above equations,

$$I_{cor} = \mathrm{K\ d}\ T_{sample+cell}\left(\frac{d\Sigma(Q)}{d\Omega}\right)_{sample} \qquad (6)$$

The instrumental scale factor, K, will be determined from a measurement of the attenuated direct beam intensity,

$$I_{direct} = T_{atten}\,\phi\,\mathrm{A}\,\Delta\Omega\,\varepsilon\,t = T_{atten}\,\mathrm{K} \qquad (7)$$

where T_{atten} is the transmission of a calibrated attenuator.

V. DATA ANALYSIS

Part I:
The objective of this part is to characterize the structure of the self-assembled aggregate. Since the volume fraction of lipid in solution is about 0.05, the first question to ask is whether it is reasonable to analyze the scattering in terms of randomly oriented, non interacting particles (so we can neglect the structure factor S(Q)=1). (Remember that the lipids are zwitterionic and carry a mean charge equal to zero). Is the concentration used high enough that the particles feel the presence of neighboring particles??
In order to answer these questions, two lipids mixtures will be dissolved in pure D2O and in 0.2M NaCl in D2O.
Scattering curves will be compared and a conclusion will be drawn.

Part II:
Once part I resolved, can we get an estimate of the size of the aggregate??

Since the lipid volume fraction in our sample is low, it is reasonable to analyze the scattering in terms of randomly oriented, non-interacting particles (in this case, we

neglect the structure factor S(Q) = 1). In this so-called dilute limit, the particles scatter independently, and the total scattering is the sum of the scattered from each particle. The measured intensity (corrected for background and put on an absolute scale) can be expressed as

$$\frac{d\Sigma(Q)}{d\Omega} = (\rho_p - \rho_w)^2 V_p^2 N_p P(Q), \quad (8)$$

where ρ_p and ρ_w are the SLDs of the particles and the D_2O (solvent), respectively; V_p is the mean particle volume, and N_p is the number of particles per unit volume. $P(Q)$ is the scattering form factor for the particles,

$$P(Q) = \left| \frac{1}{V_p} \int_{V_p} e^{i\vec{Q}\cdot\vec{r}} d\vec{r} \right|^2, \quad (9)$$

the square of the Fourier transform of the particle shape.

In the limit $Q \to 0$, the above expression (9) becomes for randomly oriented particles

$$I(Q) \propto \exp(-Q^2 R_g^2 / 3). \quad (10)$$

The above equation is an example of Guinier's Law which is valid only for $Q R_g \leq 1$, where R_g is the radius of gyration of the particle. **Where for a homogenous sphere, $R_g^2 = 3R^2/5$, for a cylinder, $R_g^2 = L^2/12+d^2/8$, and for an ellipsoid, $R_g^2 = (a^2+b^2+c^2)/5$.** This expression is easy to use and allows one to quickly extract the radius of gyration of particles in the low Q region by plotting *ln(I)* versus Q^2.

Part III:

Particle Volume Fraction Determined from Invariant or I(0):

- For all two phase systems having uniform scattering length densities in each phase, the volume fraction ϕ can be determined from the integration of the scattering over all q

$$\phi(1-\phi) = \frac{Q_I}{2\pi^2 \Delta\rho^2} \quad (11)$$

where the invariant is determined by

$$Q_I \equiv \int_0^\infty q^2 \frac{d\Sigma}{d\Omega}(q) dq \quad (12)$$

- For dilute systems, and for particle with an uniform scattering length density, the forward scattering is simply:

$$\frac{d\Sigma}{d\Omega}(0) = \phi V_P \Delta\rho^2 \quad (13)$$

where ϕ is the volume fraction of particles, V_P is the average particle volume, and $\Delta\rho^2$ is the scattering length density contrast squared.

Determination of the specific surface area:

The specific surface area is determined from small angle scattering data using the Porod's approximation:

$$\lim_{Q\to\infty} I(Q) = 2\pi\,\Delta\rho^2\, S/Q^4 \qquad (14)$$

where *S* is the surface area per unit volume.

Part IV:

Determination of the shape of the self-assembled aggregate:

In order to determine the structure of these aggregates, it is necessary to analyze the full scattering curve over the entire Q range and compare it to different scattering models. The NIST Igor SANS analysis package offers a wide variety of models of scattered intensities as well as help files including the original reference for the models and details of the calculation. Model functions can easily be plotted with the experimental measured data for quick comparison.

Once the adequate model is selected, Igor's non linear fitting routine will be used to fit the data. Sample polydispersity, instrumental resolution and the incoherent scattering from the sample, as pointed out in Section II.3 will have then to be taken into account. The later one will be done by including a constant as a fitting parameter to represent the featureless incoherent scattering. In the appendix, we briefly present the undesirable effects of sample polydispersity, resolution smearing, multiple scattering and particle-particle interaction on the scattering profile of simple solution of spheres. Those effects apply to any type of scattering and it is important to be aware of their consequences.

Part V:

Determination of the internal structure of the self-assembled aggregate:

The results of the previous sections should have led us to the characterization of the shape of the aggregate. Now we will try to determine the distribution of the lipids within the aggregate by making SANS measurements on samples with a strong contrast between the lipids i.e. mixtures of deuterated DMPC and hydrogenous DHPC at the same ratio and concentration studied previously. The SLD of d-DMPC is now close to that of the deuterated solvent and the main scattering will come from the hydrogenous DHPC. In doing so, the internal structure of the aggregate can be resolved and the question concerning total lipid mixture or total lipid segregation will be answered. Here again we will rely on scattering models to unambiguously determine the final aggregate structure (Fig. 5).

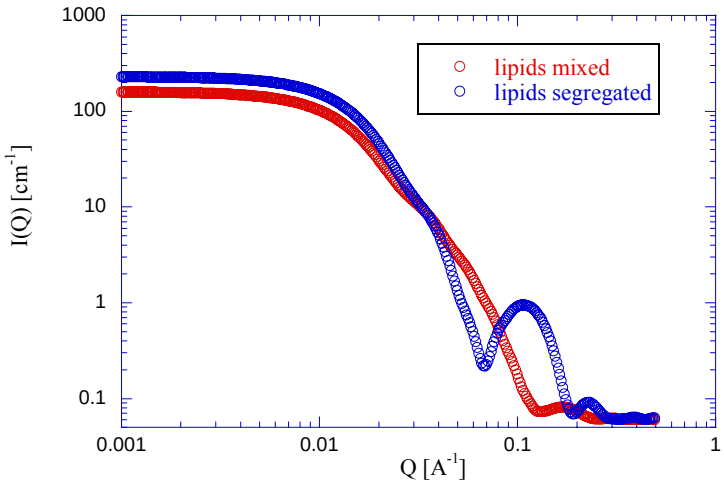

Figure 5: Scattering from a fully mixed or fully segregated mixture of d-DMPC and h-DHPC lipids in deuterated solvent with their corresponding schematic structure.

Appendix:

Polydispersity:

In practice, colloidal particles are never identical, there is always a distribution in size due to synthesis methods. In order to take into account these "imperfections", a polydisperse sphere model (called polycore model in the SANS fitting package) is proposed for solution of spheres.
The form factor *P(Q)* of polydisperse sphere is defined by:

$P(Q) = \int_0^\infty Sch(r) P_1(Q,r) dr$ where $Sch(r)$ is the Schultz distribution (polydispersity in size) which is both physically realistic as well as mathematically tractable and where $P_1(Q,r)$ is the single form factor of a sphere:

$$P_1(Q,r) = \left[\frac{3(\sin Qr - Qr\cos Qr)}{(Qr)^3} \right]^2$$

These analytical expressions can be found in the help notes of the SANS analysis package. In figure 6, we give an example of how a polydispersity in size affect the scattering data from an ideal sphere form factor

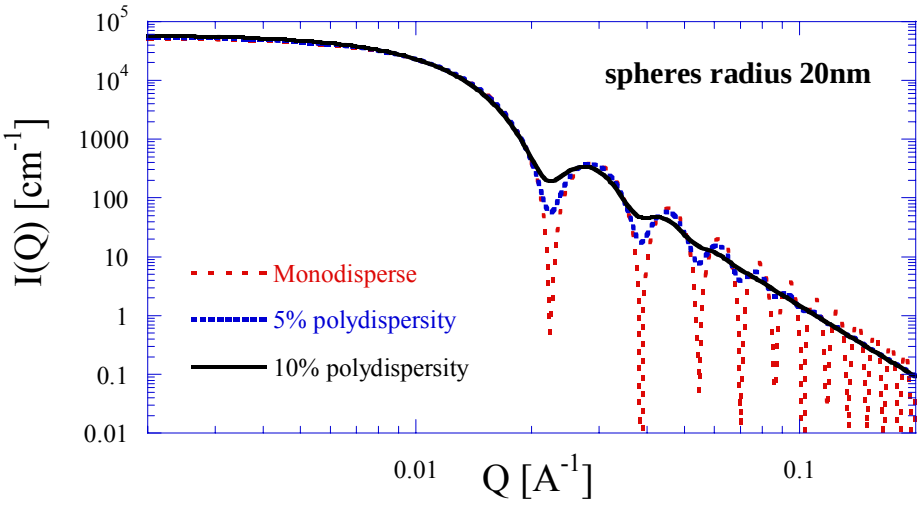

Figure 6: Effect of size polydispersity on scattering curves from spheres

Particle-particle interaction:

As explained in equation (8) the scattering intensity is proportional to the scattering contrast and particle volume fraction. So high particle content will give higher count rate and then shorter accumulation time. However, particle-particle interactions will dramatically alter the scattering curve (Figure 7), leading inexact values for radius of gyration and sample polydispersity.

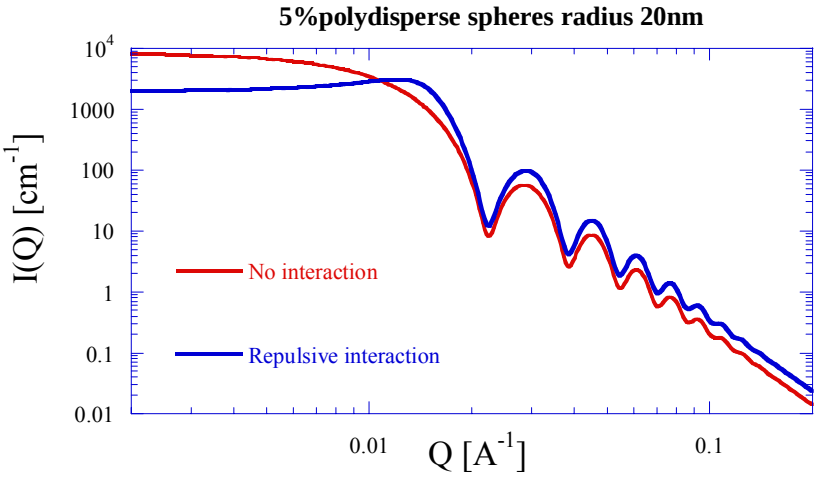

Figure 7: Effect of particle-particle interactions on scattering curves from spheres

Multiple scattering:

Multiple scattering (a neutron scatters more than once in the sample) can also dramatically alter the scattering curve

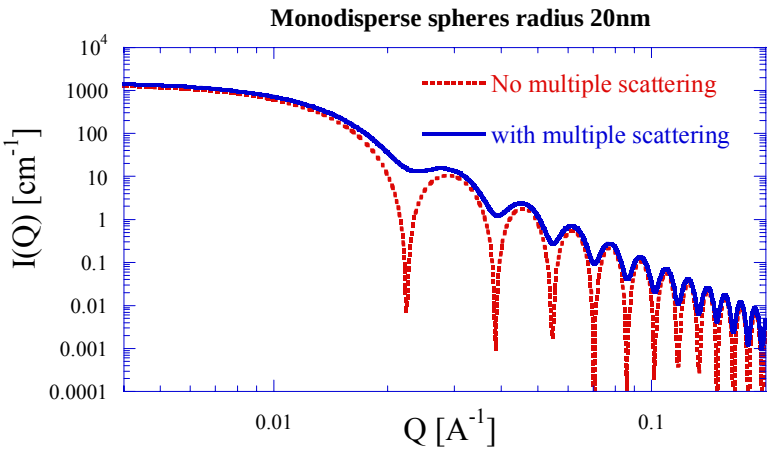

Figure 8: Effect of multiple scattering on scattering curves from spheres

Instrument resolution:

Another limiting factor to observe the minima of the form factor is the instrument resolution. Size and divergence of the beam, wavelength distribution and detector pixel size will contribute to smear the ideal sample scattered intensity and will have important influence on the measured scattering data. Figure 8 shows such an example.

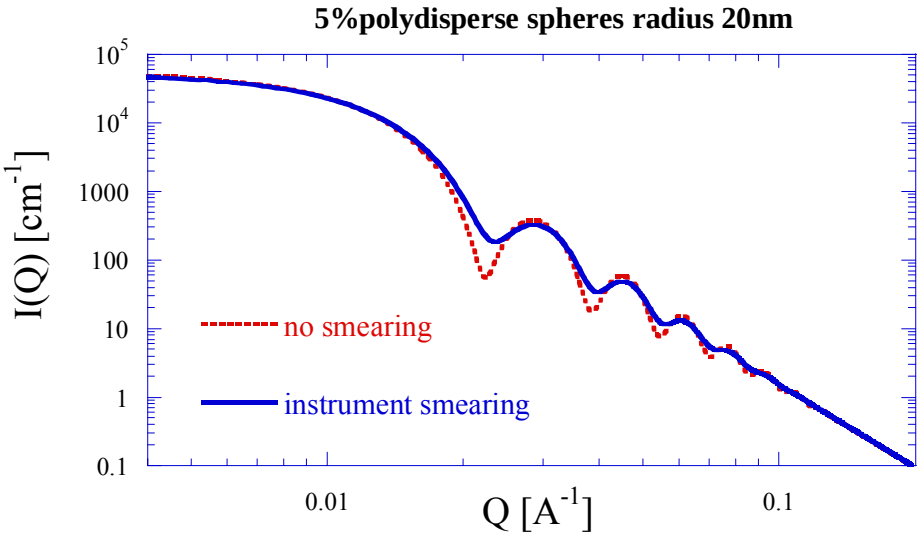

Figure 8: effect of instrumental resolution on scattering curves from 5% polydisperse spheres

In conclusion, you have to be very careful when performing a SANS experiment if you want to quantitatively explain your measurements.

VI. REFERENCES AND OTHER RESOURCES

[1] Katsaras J., Harroun T.A., Pencer J., Nieh M-P. 2005. "Bicellar" lipid mixtures as used in biochemical and Biophysical studies. *Naturwissenschaften*, 92, 355-366

[2] Marcotte I., Auger M. 2005. Bicelles as Model membranes for solid and solution-state NMR studies of Membrane proteins. *Concepts in Magnetic Resonance Part A*, 2005, Vol. 24A (1) 17-37

[3] Faham S., Bowie, J. 2002 Bicelle crystallization: A new method for crystallizing membrane proteins yields a monomeric bacteriorhodopsin structure. *J. Mol. Biol*, 316, 1-6

[4] White S., H. 2004. The progress of membrane protein structure determination. *Protein Sci.*, 13(7):1948-9.
Also, http://blanco.biomol.uci.edu/Membrane_Proteins_xtal.html

[5] V.F. Sears, *Neutron News*, Vol. 3, No. 3, p 26 (1992).